SECURITY CLASSIFICATION OF THIS PAGE *(When Data Entered)*

REPORT DOCUMENTATION PAGE

READ INSTRUCTIONS BEFORE COMPLETING FORM

1. REPORT NUMBER: AFOSR-TR- 89-0457
2. GOVT ACCESSION NO.
3. RECIPIENT'S CATALOG NUMBER

4. TITLE *(and Subtitle)*: Solving the Brightness-From-Luminance Problem: A Neural Architecture for Invariant Brightness Perception
5. TYPE OF REPORT & PERIOD COVERED: Interim report
6. PERFORMING ORG. REPORT NUMBER

7. AUTHOR(s): Stephen Grossberg and Dejan Todorović

8. CONTRACT OR GRANT NUMBER(s): ~~AFOSR~~ F49620-86-C-0037, ~~AFOSR~~ F49620-87-C-0018

9. PERFORMING ORGANIZATION NAME AND ADDRESS: Center for Adaptive Systems, Department of Mathematics, Boston University, Boston, MA 02215

10. PROGRAM ELEMENT, PROJECT, TASK AREA & WORK UNIT NUMBERS: 61102F, 21313/A5

11. CONTROLLING OFFICE NAME AND ADDRESS: AFOSR Life Sciences Directorate, Bolling Air Force Base, Washington, DC 20332 NL
12. REPORT DATE: February 1989
13. NUMBER OF PAGES: 38
14. MONITORING AGENCY NAME & ADDRESS *(if different from Controlling Office)*: Same as 11
15. SECURITY CLASS. *(of this report)*: Unclassified
15a. DECLASSIFICATION/DOWNGRADING SCHEDULE

16. DISTRIBUTION STATEMENT *(of this Report)*: Unlimited

17. DISTRIBUTION STATEMENT *(of the abstract entered in Block 20, if different from Rep...)*

18. SUPPLEMENTARY NOTES: To appear in Connectionist Modeling and Brain Function: The Developing Interface, S.J. Hanson and C. Olson (Eds.) Cambridge, MA: MIT Press, 1989

19. KEY WORDS *(Continue on reverse side if necessary and identify by block number)*: Neural Network, Vision, Brightness Perception, Discounting the Illuminant, surface recovery.

20. ABSTRACT *(Continue on reverse side if necessary and identify by block number)*

DD FORM 1 JAN 73 1473 EDITION OF 1 NOV 65 IS OBSOLETE

SECURITY CLASSIFICATION OF THIS PAGE *(When Data Entered)*

10 MAR 1989

SOLVING THE BRIGHTNESS-FROM-LUMINANCE PROBLEM: A NEURAL ARCHITECTURE FOR INVARIANT BRIGHTNESS PERCEPTION

Stephen Grossberg†
Center for Adaptive Systems
Boston University
111 Cummington Street
Boston, MA 02215

and

Dejan Todorović
Univerzitet u Beogradu
Laboratorija za Eksperimentalnu Psihologiju
Cika Ljubina 18–20
11000 Beograd
Yugoslavia

To appear in

Connectionist Modeling and Brain Function: The Developing Interface
S.J. Hanson and C. Olson (Eds.)
Cambridge, MA: MIT Press, 1989

† Supported in part by the Air Force Office of Scientific Research (~~AFOSR~~ F49620-86-C-0037 and ~~AFOSR~~ F49620-87-C-0018), the Army Research Office (ARO DAAL03-88-K-0088), and the National Science Foundation (NSF IRI-87-16960).

Acknowledgements: We wish to thank Cynthia Suchta and Carol Yanakakis for their valuable assistance in the preparation of the manuscript.

The spatial distribution of light that constitutes the input to our eyes is the foundation of all visual functions, such as perception of brightness, color, texture, form, and 3-D organization. The perception of brightness may perhaps appear to be the simplest of all functions: the most natural initial explanation of why surface A appears brighter than surface B is that more light arrives into our eyes from surface A than from B. However, as we will show in the following, the relation of luminance (which is a physical variable involving the amount of light energy arriving at the retina) and brightness (which is a psychological variable denoting perceived intensity of light) is much more complicated.

The brightness-from-luminance problem is the following: find the mapping that transforms any given spatial distribution of luminance into the corresponding spatial distribution of brightness. The problem is generally solved for the simple visual situation involving a bright patch on a dark background. Increasing the luminance of the patch causes it to look increasingly brighter, but in a nonlinear manner. The function is negatively accelerated, and the debate is only whether it is mathematically better described as a logarithm (Fechner, 1889) or as a power function (Stevens, 1957).

In more complicated visual situations containing several surfaces, their brightnesses may be predicted by taking logarithms, or power functions, of their luminances. This prediction will be wrong, and there will be a luminance-brightness mismatch, in two types of cases. They correspond to the two ways in which a one-to-one relation such as the power function can be violated (Todorović, 1987). On the one hand, there are cases in which different luminances can induce the same brightness percept. On the other hand, there are converse cases in which surfaces of the same luminance can appear differently bright. These two types of cases are best exemplified by brightness contrast and brightness constancy, two classical phenomena of brightness perception.

Brightness constancy refers to the fact that surfaces of the same reflectance (same ratio of reflected to incoming light) tend to be perceived as approximately equally bright, even under unequal illumination (Arend and Reeves, 1986; Katz, 1935). For example, two identical pieces of gray paper are perceived as approximately equally bright, whether in sunlight or in shadow, whether directly under a lamp or in a dark corner of the room. Being differently illuminated, but having the same reflectance, the two pieces of paper have different luminance (which is the product of illumination and reflectance). Their approximately equal brightness is often thought to be due to their equal reflectance. It is assumed that in the percept of brightness the visual system in some way discounts the illumination and recovers the reflectance. Perceptual brightness constancy, then, is a reflection of physical reflectance constancy: the ratio of reflected to incoming light does not depend on the intensity of incoming light. In this approach, the brightness-from-luminance problem reduces to the reflectance-from-luminance problem (Horn, 1974; Hurlbert, 1986; Land, 1977, 1986).

A difficulty for such reflectance theories of brightness is that if they are completely successful (in recovering reflectance) than they must be wrong. This is because surfaces of equal reflectance do not always appear equally bright, and any theory which predicts that they do misses an important aspect of brightness perception. Brightness contrast is the prime example of such phenomena: put two equal pieces of gray paper under equal illumination but place them on differently luminant backgrounds. Then the gray piece surrounded by the black background will look brighter than the piece on the white background. This effect of contextual dependence of brightness, where surfaces of equal luminance and reflectance look differently bright, was already known to Leonardo da Vinci, and was seriously studied in the 19th century. More recently, a host of related phenomena were discovered, such as the Hermann grid (Spillmann and Levine, 1971), the Koffka-Benussi ring (Koffka, 1935), brightness assimilation (Helson, 1963), the Wertheimer-Benary figure (Benary, 1938), and others.

An attractive phenomenon of this type is the Craik-O'Brien-Cornsweet Effect (COCE)

(Cornsweet, 1970; see Todorović (1987) for a review). One version of the COCE is presented in Figure 1. Readers unfamiliar with this effect might suppose that, since the left rectangle is brighter than the right rectangle, it is also the more luminant one. However, the luminance of the two rectangles is actually identical, except for a luminance cusp overshoot at the left flank and a luminance cusp undershoot at the right flank of the midline (see Figure 6a). The illusory nature of the phenomenon is most easily demonstrated by the occlusion of the contour region. Placing a pencil or a piece of wire vertically across the midline in Figure 1 causes the two rectangles to appear equally bright.

Figure 1

To summarize, there are at least two factors that make the relation of brightness and luminance a problem: illumination discounting and contextual dependence. We will now present a neural network architecture that deals with both issues. The model generalizes to two dimensions the types of processes that Cohen and Grossberg (1984) used to simulate 1-D brightness phenomena. This generalization conjoins processing concepts and mechanisms from Cohen and Grossberg (1984) and those from Grossberg and Mingolla (1985, 1987). For a detailed presentation of the theory and simulations please consult Grossberg and Todorović (1988). The theory suggests that two parallel contour-sensitive processes interact to generate a brightness percept. The Boundary Contour (BC) System, comprised by several interacting networks, synthesizes an emergent boundary segmentation from combinations of oriented and unoriented scenic elements. The Feature Contour (FC) System triggers a diffusive filling-in of featural quality within perceptual domains whose boundaries are determined by output signals from the BC System. Neurophysiological and anatomical data from the lateral geniculate nucleus and visual cortex which have been analysed and predicted by the theory are summarized in Grossberg (1987a, 1987b).

THE MODEL

Figure 2 provides an overview of the neural network model that we have analysed. The model has six levels depicted as thick-bordered rectangles numbered from 1 to 6. Levels 1 and 2 are preprocessing levels prior to the BC and FC Systems. Output signals from Level 2 generate inputs to both of these systems. Levels 3–5 are processing stages within the BC System. Level 6, which models the FC System, receives inputs from both Level 2 and Level 5.

Figure 2

Each level contains a different type of neural network. The type of network is indicated by the symbol inside the rectangle. The symbols provide graphical mnemonics for the processing characteristics at a given level, and are used in the figures that present the computer simulations of the 2-D implementation of the model. The arrows connecting the rectangles depict the flow of processing between the levels. The type of signal processing between different levels is indicated inside thin-bordered insets attached by broken lines to appropriate arrows, and coded by letters A through E. The sketch inside the inset coded F depicts the complex interactions between Levels 2, 5, and 6. The mathematical structure of the model is presented in the Appendix.

The first level of the model consists of a set of units that sample the luminance distribution. In the 1-D version of the model the units are arranged on a line; in the 2-D version they form a square grid. Level 2 contains two networks with units that model on-cells and off-cells. These are neurons with concentric antagonistic receptive fields found at early levels of the visual system. In Figure 2 the on-cells are symbolized with a white center and a black annulus, and the off-cells with a black center and a white annulus. The 1-D cross-sections of these fields are sketched in insets A and B of Figure 2. In two dimensions, these

profiles have the shapes of sombreros for on-units, and inverted sombreros for off-units. The activity level of such cells correlates with the size of the center-surround luminance contrast. Due to the postulated shunting interaction (see Appendix), the cells are sensitive to relative contrast in a manner approximating a Weber law (Grossberg, 1983). In addition, the cells are tuned to display non-negligible activity levels even for homogeneous stimulation, as do retinal ganglion cells (Enroth-Cugell and Robson, 1984). This property enables such a cell to generate output signals that are sensitive to both excitatory and inhibitory inputs.

Level 3 consists of units that share properties with cortical simple cells. The symbol for these units in Figure 2 expresses their sensitivity to luminance contrast of a given orientation and a given direction of contrast. Inset C depicts the 1-D cross-section of the receptive field of such units, taken with respect to the network of on-cells. In our 2-D simulations, the function we used to generate this receptive field profile was the difference of two identical bivariate Gaussians whose centers were shifted with respect to each other. A similar formalization was used by Heggelund (1981a, 1981b, 1985). In our current implementation, Level 3 units are activated by Level 2 on-units.

Level 3 units are sensitive to oriented contrasts in a specific direction-of-contrast, as are cortical simple cells. However, complex cells sensitive to contrasts of specific orientation regardless of polarity are also well-known to occur in striate cortical area 17 of monkeys (Hubel and Wiesel, 1968) and cats (Hubel and Wiesel, 1962). See Grossberg (1987a) for a review of relevant data and related models. Units fulfilling the above criteria populate Level 4 of our network. Inset D in Figure 2 depicts the construction of Level 4 cells out of Level 3 cells. The mathematical specification is similar to the one used by Grossberg and Mingolla (1985a, 1985b). The symbol for Level 4 units expresses their sensitivity to oriented contrasts of either direction. Each Level 4 unit at a particular location is excited by two Level 3 units at the corresponding location having the same axis of orientation but opposite direction preference. Thus the twelve Level 3 types of units give rise to six Level 4 unit types. Interestingly, several physiological studies have found that the simple cells outnumber the complex cells in a ratio of approximately 2 to 1, and that complex cells have a higher spontaneous activity level than simple cells (Kato, Bishop, and Orban, 1978). Both of these properties are consistent with the proposed circuitry.

In the simulations presented in this paper, we have used a simplified version of the BC System. The final output of this system is found at Level 5 of the model. A unit at a given Level 5 location can be excited by any Level 4 unit located at the position corresponding to the position of the Level 5 unit. A Level 4 unit excites a Level 5 unit only if its own activity exceeds a threshold value. The pooling of signals sensitive to different orientations is sketched in inset E and expressed in the symbol for Level 5 in Figure 2. This pooling may, in principle, occur entirely in convergent output pathways from the BC System to the FC System, rather than at a separate level of cells within the BC System.

Network activity at Level 6 of our model corresponds to the brightness percept. Level 6 is part of the FC System, which is composed of a syncytium of cells. This is a regular array of intimately connected cells such that contiguous cells can easily pass signals between each other's compartment membranes, possibly via gap junctions (Piccolino, Neyton, and Gerschenfeld, 1984). Due to the syncytial coupling of each cell with its neighbors, the activity can rapidly spread to neighboring cells, then to neighbors of the neighbors, and so on. Because the spreading, or filling-in, of activation occurs via a process of diffusion, it tends to average the activation that is triggered by an FC input from Level 2 across the Level 6 cells that receive this spreading activity. The inset labeled F in Figure 2 summarizes the three factors that influence the magnitude of activity of units at Level 6. First, each unit receives bottom-up input from Level 2, the field of concentric on-cells. Second, there are lateral connections between neighboring units at Level 6 that define the syncytium, which supports within-network spread of activation, or filling-in. Third, this

lateral spread is modulated by inhibition from Level 5 in the form of BC signals capable of decreasing the magnitude of mutual influence between neighboring Level 6 units. The net effect of these interactions is that the FC signals generated by the concentric on-cells are diffused and averaged within boundaries generated by BC signals.

The idea of a filling-in process has been invoked in various forms by several authors in discussions of different brightness phenomena (Davidson and Whiteside, 1971; Fry, 1948; Gerrits and Vendrick, 1970; Hamada, 1984; Walls, 1954). In the present model, this notion is fully formalized, related to a possible neurophysiological foundation, tied in with other mechanisms as a part of a more general vision theory, and applied in a systematic way to a variety of brightness phenomena.

1-D SIMULATIONS

The model described in the preceding section was implemented in a 1-D and a 2-D version. Simulations from both versions will be presented. All graphical depictions of the 1-D simulations contain four distributions: the stimulus luminance distribution (Level 1), the on-unit distribution (Level 2), the output of the BC System (Level 5), and the syncytium distribution (Level 6), which corresponds to the predicted brightness distribution. Cohen and Grossberg (1984) presented their simulation of various brightness phenomena in a similar format. The graphs of the four distributions were scaled separately; that is, each was normalized with respect to its own maximum.

We begin with the simulation of a simple visual situation whose purpose is to set the context for the following simulations. The Level 1 luminance distribution, labeled Stimulus, is presented in the bottom graph of Figure 3. It portrays the horizontal cross-section of an evenly illuminated scene containing two equally luminant homogeneous patches on a less luminant homogeneous background. The Level 2 reaction of on-units to such a stimulation, labeled Feature, illustrates the cusp-shaped profiles that correspond to luminance discontinuities. The four boundary contours formed at Level 5 of the system are labeled Boundary. Finally, the top graph, labeled Output, presents the Level 6 filled-in activity profile that embodies the prediction of a brightness distribution qualitatively isomorphic with the luminance distribution. This percept contains two homogeneous, equally bright patches on a darker, homogeneous background.

Figure 3

What happens when the two-patch scene is unevenly illuminated? Figure 4 presents a luminance distribution that mimics the effects of a light source off to the right side of the scene. The luminance profile is now tilted, and the right patch has more average luminance than the left patch. Inspection of the Output reveals that the model exhibits brightness constancy. It predicts a percept whose structure is very similar to the one in the preceding, evenly illuminated scene. One factor that contributes to this outcome is the ratio-processing characteristic of the Level 2 units. Although the absolute luminance values in the stimulus distribution in Figures 3 and 4 are different, the ratio of the lower to higher luminance across all edges in both distributions is 1 : 3. Therefore, the activity profiles of Level 2 on-units are very similar in both cases, as is the activity in all subsequent processing stages. The consequence is that the illuminant is effectively discounted.

Figure 4

The importance of luminance ratios for brightness perception was stressed by Wallach (1948, 1976). He found that if one region was completely surrounded by another, the brightness of the inner region was predominantly influenced by the size of the ratio of its luminance to the luminance of the surround. Our model provides a mechanical explanation

of why the ratio principle is effective in such situations. In addition, the model is applicable to more general visual situations in which multiple regions have multiple neighbors, and it provides perceptually correct predictions in situations in which the ratio principle fails.

Figure 5 shows how the model handles brightness contrast. This luminance profile characterizing the favorite textbook example of this phenomenon is depicted as the Stimulus. The luminance distribution is similar to the one in Figure 3 in that it contains two patches of medium luminance level. However, the left patch is positioned on a lower luminance background, and the right patch on a higher luminant one. Inspection of the Output in Figure 5 reveals that the prediction of the model is in accord with the perceptual fact that the patch on the dark background looks brighter than the patch on the bright background. Note that the central portions of the on-units profiles (Level 2) that correspond to the stimulus patches in Figure 5 have the same activity magnitude. Hence, these activity profiles cannot account for the difference in the appearance of the patches. However, the filled-in activity patterns within each region of the Level 6 output in Figure 5 are different and homogeneous.

Figure 5

In addition to the classical brightness phenomena, the model also explains a variety of more recently studied effects. Grossberg and Todorović (1988) presented 1-D simulations of experimental findings by Arend, Buehler, and Lockhead (1971), Arend and Goldstein (1987), Shapley (1986), and Shapley and Reed (1986). In all cases, brightness relationships found in the psychophysical experiments match those predicted by the model.

2-D SIMULATIONS

Although a 1-D model suffices for some brightness effects, others can only be profitably studied and simulated by means of a 2-D architecture. The graphical depictions of our simulations consist of 30×30 or 40×40 arrays of circular symbols of different types. As noted, the type of a symbol serves as a mnemonic of the type of the unit it represents. The size of the radius of a symbol represents the magnitude of its activity. The particular sizes of the circular symbols on the printed page were chosen according to the following scaling procedure: the unit or units with the maximum activity are represented with circles whose radius is equal to half the distance between the centers of two neighboring units on the grid; the remaining circles are scaled proportionally.

Figure 6 shows how the model handles the COCE. Figure 6a is a 2-D stimulus representation (Level 1) depicting the standard case of the COCE presented in Figure 1. Figure 6b describes the activity pattern across the field of circular concentric on-units (Level 2). Note that the middle portions of the left and right region corresponding to the two rectangles have approximately the same level of activity. However, there is an overshoot at all four edges of the left region, but only at three edges of the right region. Thus, on average there is more activity within the left than within the right region. Figure 6c describes the activity pattern across the field of boundary contour units which delineate two rectangular compartments (Level 5). The activity pattern at Level 2 generates a filling-in reaction at Level 6 within these boundary compartments. Figure 6d, which should be compared with the percept in Figure 1, presents this final filled-in activity pattern. The activity is uniformly higher in the left rectangle than in the right one, because on the left side there is a larger total amount of Level 2 activity than on the right side, but they diffuse within the same-sized compartments. See Grossberg and Todorović (1988) for simulations of several variations of COCE presented by Todorović (1987).

Figure 6

The interactions of the BC System and the filling-in process are well illustrated in Figure 7, which presents the simulation of the Koffka-Benussi ring (Berman and Leibowitz, 1965; Koffka, 1935). The version that we simulate uses a rectangular annulus. The annulus has an intermediate luminance level and is superimposed upon a bipartite background of the same type as in the classical brightness contrast condition, with one half having a high luminance level and the other half a low luminance level (Figure 7a). The percept of such a stimulus is that the annulus is approximately uniform in brightness, although the right and the left halves of the annulus exhibit some brightness contrast. This percept corresponds to the Level 6 activity profile in Figure 7b.

Figure 7

The brightness distribution in the percept can be changed by the introduction of a narrow black line dividing the stimulus vertically into two halves. Figure 7c presents the new stimulus distribution. In the percept, as in the Level 6 activity profile (Figure 7d), the annulus is now divided into two regions with homogeneous but different brightnesses that are in accord with brightness contrast. These effects depend critically upon interactions between contrast, boundaries, and filling-in in the model. In the unoccluded Koffka-Benussi ring, the annular region at Level 6 is a single connected compartment within which diffusion of activity proceeds freely. The opposite contrast due to the two halves of the background are effectively averaged throughout the annular region, although a residual effect of opposite contrast remains. The introduction of the occluding boundary (Figure 7c) divides the annulus into two smaller compartments (Figure 7d). The different contrasts are now constrained to diffuse within these compartments, generating two homogeneous regions of different brightness. See Grossberg and Todorović (1988) for additional 2-D simulations of brightness phenomena of the Hermann grid and the Kanizsa-Minguzzi anomalous brightness differentiation.

The last set of simulations that we present here was done on a set of images popularized by E. Land, who named them after Piet Mondrian, the Dutch painter. They consist of randomly arranged collages of homogeneous surfaces of different reflectances. We use here an example similar to the one presented by Shapley (1986). Consider the two squares in Figure 8a, the first near the top left corner, and the second near the bottom right corner, which have the same size and luminance. Despite these equalities, the filled-in activity profile of the upper square is more intense than that of the lower square, corresponding to the percept that the upper square is brighter. This brightness difference is due to the following combination of factors in our model. The luminance of the regions surrounding the two squares were chosen such that, on average, the upper square is more luminant than its surround, and the lower square is less luminant than its surround. In consequence, as can be seen in Figure 8b, more Level 2 on-unit activity is present within the region corresponding to the upper square. The on-unit activity diffuses within the compartments delineated by the BC's (Figure 8c). Thus, in the filled-in upper square of Figure 8d, a larger amount of activity is spread across the same area as in the lower square, thereby explaining the final brightness difference.

Figure 8

Figure 9

Figure 9a presents a Mondrian that is illuminated by a gradient of light that decreases linearly across space from the lower right corner of the figure. The upper square now exhibits, on average, less luminance than the lower square. Despite this fact, the filled-in activity profile of the upper square at Level 6 is more intense than that of the lower square (Figure 9d). Figures 8b and 9b, 8c and 9c, and 8d and 9d are, in fact, virtually indistinguishable. Thus this simulation exhibits brightness constancy by effectively discounting the illuminant, while at the same time retaining the effect of generalized brightness contrast. We call this *contrast constancy*, an effect which, to our knowledge, has not yet been

psychophysically tested. This result does not, however, imply that complete discounting will occur in response to all combinations of achromatic and chromatic images, illuminants, and bounding regions (Arend and Reeves, 1986). The systematic analysis of all these factors remains for future research.

DISCUSSION

The computer implementation of the model described in this paper has a limited domain of application since it deals only with monocular achromatic brightness effects. Extensions into the chromatic and the binocular domains have been described in Grossberg (1987a, 1987b). Brightness can also be influenced by emergent segmentations that are not directly induced by image contrasts, as in Kanizsa's illusory triangle, the Ehrenstein illusion, and neon color spreading effects. These and related grouping and segmentation effects have been discussed by Grossberg and Mingolla (1985a, 1985b). Their implementation includes a version of the BC System in which emergent segmentations can be generated through lateral interactions between oriented channels. Such interactions may play a role in the orientation-sensitive brightness effects reported by McCourt (1982), Sagi and Hochstein (1985), and White (1979). The implementation in this paper also omits possible effects of multiple scale processing, as the receptive fields of all units within a network were assumed to have a single receptive field size. Units of multiple sizes may be involved in the explanation of classical brightness assimilation (Helson, 1963). Grossberg and Mingolla have studied the role of multiple scales in the perception of 3-D smoothly curved and shaded objects. A number of depth-related effects, such as the phenomena of transparency (Metelli, 1974) and proximity-luminance covariance (Dosher, Sperling, and Wurst, 1986) have been discussed by Grossberg (1987a, 1987b). The model in its current form also does not treat the temporal variation of brightness due to image motion (Cavanagh and Anstis, 1986; Todorović, 1983, 1987) or stabilization (Krauskopf, 1963; Pritchard, 1961; Yarbus, 1967). Finally, the application of the model to natural noisy images has yet to be accomplished.

In sum, the system described in this paper does not attempt to explain the complete gamut of brightness phenomena. These limitations are not, however, insurmountable obstacles; rather, they point to natural extensions of the model, many of which have been discussed and implemented in related work. However, even the processing of brightness in monocular, achromatic, static, noise-free images is full of surprising complexities. Only a model capable of handling these basic phenomena can be a foundation upon which still more complex effects can be explained. Not much computationally oriented work has been devoted to these fundamental aspects of visual perception. Several contemporary algorithms were influenced by Land's seminal work (Blake, 1985; Frisby, 1979; Horn, 1974; Hurlbert, 1986). Other computational models have provided alternative approaches to the analysis of filling-in (Arend and Goldstein, 1987; Hamada, 1984). Our model has been used to simulate a much larger set of brightness data, and includes mechanistic explanations of classical longstanding phenomena described in every review of brightness processing, recently discovered but unexplained data, and predictions of yet untested phenomena, including predictions of testable patterns of physiological activation.

APPENDIX

The equations underlying the model are based on and are an extension of work by Grossberg (1983), Cohen and Grossberg (1984) and Grossberg and Mingolla (1985b, 1986a). The exposition follows the description of Levels in Figure 2. Only the two-dimensional versions of the equations are presented. The one-dimensional forms can be derived by straightforward simplifications. The two-dimensional simulations were performed on a 30×30 lattice or a 40×40 lattice. The one-dimensional simulations involve 256 units.

Level 1: Gray-Scale Image Description

We denote by I_{ij} the value of the stimulus input at position (i, j) in the lattice. In all simulations these values varied between 1 and 9. In order to compute the spatial convolutions of Level 2 cells without causing spurious edge effects at the extremities of the luminance profile, the luminance values at the extremities were continued outward as far as necessary.

Level 2: Shunting On-Center Off-Surround Network for Discounting Illuminants and Extracting FC Signals

The activity x_{ij} of a Level 2 on-cell at position (i, j) of the lattice obeys a membrane equation

$$\frac{d}{dt}x_{ij} = -Ax_{ij} + (B - x_{ij})C_{ij} - (x_{ij} + D)E_{ij}, \tag{A1}$$

where C_{ij} (E_{ij}) is the total excitatory (inhibitory) input to x_{ij}. Each input C_{ij} and E_{ij} is a discrete convolution with Gaussian kernel of the inputs I_{pq}:

$$C_{ij} = \sum_{(p,q)} I_{pq} C_{pqij} \tag{A2}$$

and

$$E_{ij} = \sum_{(p,q)} I_{pq} E_{pqij}, \tag{A3}$$

where

$$C_{pqij} = C \exp\{-\alpha^{-2} \log 2[(p - i)^2 + (q - j)^2]\} \tag{A4}$$

and

$$E_{pqij} = E \exp\{-\beta^{-2} \log 2[(p - i)^2 + (q - j)^2]\}. \tag{A5}$$

Thus, the influence exerted on the Level 2 potential x_{ij} by input I_{pq} diminishes with increasing distance between the two corresponding locations. The decrease is isotropic, inducing the circular shape of the receptive fields. To achieve an on-center off-surround anatomy, coefficient C of the excitatory kernel in (A4) is chosen larger than coefficient E of the inhibitory kernel in (A5), but α, the radius of the excitatory spread at half strength in (A4), is chosen smaller than β, its inhibitory counterpart in (A5). In the simulations, this equation is solved at equilibrium. Then $\frac{d}{dt}x_{ij} = 0$, so that

$$x_{ij} = \frac{\sum_{(p,q)}(BC_{pqij} - DE_{pqij})I_{pq}}{A + \sum_{(p,q)}(C_{pqij} + E_{pqij})I_{pq}}. \tag{A6}$$

The denominator term normalizes the activity x_{ij}.

The off-cell potential $\overline{x}_{ij}$ at position (i,j) also obeys a membrane equation with an equilibrium value of the same form

$$\overline{x}_{ij} = \frac{\sum_{(p,q)}(B\overline{C}_{pqij} - D\overline{E}_{pqij})I_{pq}}{A + \sum_{(p,q)}(\overline{C}_{pqij} + \overline{E}_{pqij})I_{pq}} \tag{A7}$$

The duality between on-cell and off-cell receptive fields was achieved by setting

$$\overline{C}_{pqij} = E_{pqij} \tag{A8}$$

and

$$\overline{E}_{pqij} = C_{pqij}. \tag{A9}$$

The output signal from Level 2 is the nonnegative, or rectified, part of x_{ij}:

$$X_{ij} = \max(x_{ij}, 0). \tag{A10}$$

Levels 3–5 compute the Boundary Contour signals used to contain the featural filling-in process.

Level 3: Simple Cells

The potential y_{ijk} of the cell centered at position (i,j) with orientation k on the hour code in Figure 7 obeys an additive equation

$$\frac{d}{dt}y_{ijk} = -y_{ijk} + \sum_{(p,q)} X_{pq}F^{(k)}_{pqij} \tag{A11}$$

which is computed at equilibrium:

$$y_{ijk} = \sum_{(p,q)} X_{pq}F^{(k)}_{pqij} \tag{A12}$$

in all our simulations. In order to generate an oriented kernel $F^{(k)}_{pqij}$ as simply as possible, let $F^{(k)}_{pqij}$ be the difference of an isotropic kernel G_{pqij} centered at (i,j) and another isotropic kernel $H^{(k)}_{pqij}$ whose center $(i+m_k, j+n_k)$ is shifted from (i,j) as follows:

$$F^{(k)}_{pqij} = G_{pqij} - H^{(k)}_{pqij} \tag{A13}$$

where

$$G_{pqij} = \exp\{-\gamma^{-2}[(p-i)^2 + (q-j)^2]\} \tag{A14}$$

and

$$H^{(k)}_{pqij} = \exp\{-\gamma^{-2}[(p-i-m_k)^2 + (q-j-n_k)^2]\} \tag{A15}$$

with

$$m_k = \sin\frac{2\pi k}{K} \tag{A16}$$

and

$$n_k = \cos \frac{2\pi k}{K}. \tag{A17}$$

In the 2-D simulations, the number K of hour codes is 12, whereas for the 1-D simulations it is 2.

The output signal from Level 3 to Level 4 is the nonnegative, or rectified, part of y_{ijk}, namely

$$Y_{ijk} = \max(y_{ijk}, 0). \tag{A18}$$

Level 4: Complex Cells

Each Level 4 potential z_{ijk} with position (i, j) and orientation k is made sensitive to orientation but insensitive to direction-of-contrast by summing the output signals from the appropriate pair of Level 3 units with opposite contrast sensitivities; viz.,

$$z_{ijk} = Y_{ijk} + Y_{ij(k+\frac{K}{2})} \tag{A19}$$

An output signal Z_{ijk} is generated from Level 4 to Level 5 if the activity z_{ijk} exceeds the threshold L:

$$Z_{ijk} = \max(z_{ijk} - L, 0). \tag{A20}$$

Level 5: Boundary Contour Signals

A Level 5 signal z_{ij} at position (i, j) is the sum of output signals from all Level 4 units at that position; viz.,

$$Z_{ij} = \sum_k Z_{ijk}. \tag{A21}$$

Level 6 computes the filling-in process, which is initiated by Feature Contour inputs from Level 2 and contained by Boundary Contour inputs from Level 5.

Level 6: Filling-In Process

Each potential S_{ij} at position (i, j) of the syncytium obeys a nonlinear diffusion equation

$$\frac{d}{dt} S_{ij} = -M S_{ij} + \sum_{(p,q) \in N_{ij}} (S_{pq} - S_{ij}) P_{pqij} + X_{ij} \tag{A22}$$

The diffusion coefficients that regulate the magnitude of cross influence of location (i, j) with location (p, q) depend on the Boundary Contour signals Z_{pq} and Z_{ij} as follows:

$$P_{pqij} = \frac{\delta}{1 + \epsilon(Z_{pq} + Z_{ij})} \tag{A23}$$

The set N_{ij} of locations comprises only the lattice nearest neighbors of (i, j):

$$N_{ij} = \{(i, j-1), (i-1, j), (i+1, j), (i, j+1)\}. \tag{A24}$$

At lattice edges and corners, this set is reduced to the set of existing neighbors. According to equation (A22), each potential S_{ij} is activated by the on-cell output signal X_{ij} and thereupon engages in passive decay (term $-MS_{ij}$) and diffusive filling-in with its four

nearest neighbors to the degree permitted by the diffusion coefficients P_{pqij}. At equilibrium, each S_{ij} is computed as the solution of a set of simultaneous equations

$$S_{ij} = \frac{X_{ij} + \sum_{(p,q)\in N_{ij}} S_{pq} P_{pqij}}{M + \sum_{(p,q)\in N_{ij}} P_{pqij}} \qquad (A25)$$

which is compared with properties of the brightness percept.

In all simulations the following parameter values were used: $A = 1, B = 90, D = 60, \gamma = 1$. All two-dimensional simulations shared the following parameters: $C = 18, M = 1, \alpha = .25, \epsilon = 1, E = .5, \beta = 3, \delta = 300, L = 10$. All one-dimensional simulations used $C = 4, M = 10, \alpha = 1, \epsilon = 100, E = .5, \beta = 8, \delta = 100,000, L = 5$.

REFERENCES

Arend, L.E., Buehler, J.N., and Lockhead, G.R. (1971). Difference information in brightness perception. *Perception and Psychophysics*, **9**, 367–370.

Arend, L.E. and Goldstein, R.E. (1987). Lightness models, gradient illusions, and curl. *Perception and Psychophysics*, **42**, 65–80.

Arend, L.E. and Reeves, A. (1986). Simultaneous color constancy. *Journal of the Optical Society of America*, **A3**, 1743–1751.

Benary, W. (1924). Beobachtungen zu einem Experiment ueber Helligkeitskontrast. *Psychologische Forschung*, **5**, 131–142. Translated as "The influence of form on brightness contrast." In W.D. Ellis (Ed.), **A source book of Gestalt psychology**. London: Routledge and Kegan Paul, 1938.

Berman, P.W. and Leibowitz, H.W. (1965). Some effects of contour on simultaneous brightness contrast. *Journal of Experimental Psychology*, **69**, 251–256.

Blake, A. (1985). Boundary conditions for lightness computation in Mondrian world. *Computer Vision, Graphics, and Image Processing*, **14**, 314–327.

Cavanagh, P. and Anstis, S.M. (1986). Brightness shift in drifting ramp gratings isolates a transient mechanism. *Vision Research*, **26**, 899–908.

Cohen, M.A. and Grossberg, S. (1984). Neural dynamics of brightness perception: Features, boundaries, diffusion, and resonance. *Perception and Psychophysics*, **36**, 428–456.

Cornsweet, T.N. (1970). **Visual perception**. New York: Academic Press.

Davidson, M. and Whiteside, J.A. (1971). Human brightness perception near sharp contours. *Journal of the Optical Society of America*, **61**, 530–536.

Dosher, B.A., Sperling, G., and Wurst, S. (1986). Tradeoffs between stereopsis and proximitiy luminance covariance as determinants of perceived 3-D structure. *Vision Research*, **26**, 973–979.

Enroth-Cugell, C. and Robson, J.G. (1984). Functional characteristics and diversity of cat retinal ganglion cells. *Investigative Ophthalmology and Visual Science*, **25**, 250–267.

Fechner, G.T. (1889). **Elemente der Psychophysik** (2nd edition). Leipzig: Breitkopf und Härtel.

Frisby, J.P. (1979). **Seeing: Illusion, brain, and mind**. Oxford: Oxford University Press.

Fry, G.A. (1948). Mechanisms subserving simultaneous brightness contrast. *American Journal of Optometry and Archives of the American Academy of Optometry*, **25**, 162–178.

Gerrits, H.J.M. and Vendrick, A.J.H. (1970). Simultaneous contrast, filling-in process and information processing in man's visual system. *Experimental Brain Research*, **11**, 411–430.

Grossberg, S. (1983). The quantized geometry of visual space: The coherent computation of depth, form, and lightness. *Behavioral and Brain Sciences*, **6**, 625–692.

Grossberg, S. (1987a). Cortical dynamics of three-dimensional form, color, and brightness perception, I: Monocular theory. *Perception and Psychophysics*, **41**, 87–116.

Grossberg, S. (1987b). Cortical dynamics of three-dimensional form, color, and brightness perception, II: Binocular theory. *Perception and Psychophysics*, **41**, 117–158.

Grossberg, S. and Mingolla, E. (1985a). Neural dynamics of form perception: Boundary completion, illusory figures, and neon color spreading. *Psychological Review*, **92**, 173–211.

Grossberg, S. and Mingolla, E. (1985b). Neural dynamics of perceptual grouping: Textures, boundaries, and emergent segmentations. *Perception and Psychophysics*, **38**, 141–171.

Grossberg, S. and Mingolla, E. (1987). Neural dynamics of surface perception: Boundary webs, illuminants, and shape-from-shading. *Computer Vision, Graphics, and Image Processing*, **37**, 116–165.

Grossberg, S. and Todorović, D. (1988). Neural dynamics of 1-D and 2-D brightness perception: A unified model of classical and recent phenomena. *Perception and Psychophysics*, **43**, 241–277.

Hamada, J. (1984). A multistage model for border contrast. *Biological Cybernetics*, **51**, 65–70.

Heggelund, P. (1981a). Receptive field organisation of simple cells in cat striate cortex. *Experimental Brain Research*, **42**, 89–98.

Heggelund, P. (1981b). Receptive field organisation of complex cells in cat striate cortex. *Experimental Brain Research*, **42**, 99–107.

Heggelund, P. (1985). Quantitative studies of enhancement and suppression zones in the receptive field of simple cells in cat striate cortex. *Journal of Physiology*, **373**, 293–310.

Helson, H. (1963). Studies of anomalous contrast and assimilation. *Journal of the Optical Society of America*, **53**, 179–184.

Horn, B.K.P. (1974). Determining lightness from an image. *Computer Graphics and Image Processing*, **3**, 277–299.

Hubel, D.H. and Wiesel, T.N. (1962). Receptive fields, binocular interaction and functional architecture in the cat's visual cortex. *Journal of Physiology*, **160**, 106–154.

Hubel, D.H. and Wiesel, T.N. (1968). Receptive fields and functional architecture of monkey striate cortex. *Journal of Physiology*, **195**, 215–243.

Hurlbert, A. (1986). Formal connections between lightness algorithms. *Journal of the Optical Society of America*, **A3**, 1684–1693.

Kanizsa, G. and Minguzzi, G.F. (1986). An anomalous brightness differentiation. *Perception*, **15**, 223–226.

Kato, H., Bishop, P.O., and Orban, G.A. (1978). Hypercomplex and simple/complex cell classifications in cat striate cortex. *Journal of Neurophysiology*, **41**, 1071–1095.

Katz, D. (1935). **The world of colour**. London: Kegan Paul, Trench, Trubner and Co. Ltd.

Koffka, K. (1935). **Principles of Gestalt psychology**. New York: Harcourt and Brace.

Krauskopf, J. (1963). Effect of retinal image stabilization on the appearance of heterochromatic targets. *Journal of the Optical Society of America*, **53**, 741–744.

Land, E. (1977). The Retinex theory of color vision. *Scientific American*, **237**, 108–128.

Land, E. (1986). Recent advances in Retinex theory. *Vision Research*, **26**, 7–21.

McCourt, M.E. (1982). A spatial frequency dependent grating-induction effect. *Vision Research*, **22**, 119–134.

Metelli, F. (1974). The perception of transparency. *Scientific American*, **230**, 90–98.

Piccolino, M., Neyton, J., and Gerschenfeld, H.M. (1984). Decrease of gap junction permeability induced by dopamine and cyclic adenosine 3′ : 5′-monophosphate in horizontal cells of turtle retina. *Journal of Neuroscience*, **4**, 2477–2488.

Pritchard, R.M. (1961). Stabilized images on the retina. *Scientific American*, **204**, 72–78.

Sagi, D. and Hochstein, S. (1985). Lateral inhibition between spatially adjacent spatial-frequency channels? *Perception and Psychophysics*, **37**, 315–322.

Shapley, R. (1986). The importance of contrast for the activity of single neurons, the VEP and perception. *Vision Research*, **26**, 45–61.

Shapley, R. and Reid, R.C. (1986). Contrast and assimilation in the perception of brightness. *Proceedings of the National Academy of Sciences USA*, **82**, 5983–5986.

Spillmann, L. and Levine, J. (1971). Contrast enhancement in a Hermann grid with variable figure-ground ratio. *Experimental Brain Research*, **13**, 547–559.

Stevens, S.S. (1957). On the psychophysical law. *Psychological Review*, **64**, 153–180.

Todorović, D. (1983). Brightness perception and the Craik-O'Brien-Cornsweet effect. Unpublished M.A. Thesis. Storrs: University of Connecticut.

Todorović, D. (1987). The Craik-O'Brien-Cornsweet effect: New varieties and their theoretical implications. *Perception and Psychophysics*, **42**, 545–560.

Wallach, H. (1948). Brightness constancy and the nature of achromatic colors. *Journal of Experimental Psychology*, **38**, 310–324.

Wallach, H. (1976). **On perception**. New York: Quadrangle.

Walls, G. (1954). The filling-in process. *American Journal of Optometry*, **31**, 329–340.

White, M. (1979). A new effect of pattern on perceived lightness. *Perception*, **8**, 413–416.

Yarbus, A.L. (1967). **Eye movements and vision**. New York: Plenum Press.

FIGURE CAPTIONS

Figure 1. The Craik-O'Brien-Cornsweet Effect (COCE). The left rectangle looks uniformly brighter than the right one. They have identical luminance, except for the cusp-shaped profile of their shared vertical border (from Todorović, 1987).

Figure 2. Overview of the model. The thick-bordered rectangles numbered from 1 to 6 correspond to the levels of the system. The symbols inside the rectangles are graphical mnemonics for the types of computational units residing at the corresponding model levels. The arrows depict the interconnections between the levels. The thin-bordered rectangles coded by letters A through E represent the type of processing between pairs of levels. Inset F illustrates how the activity at Level 6 is modulated by outputs from Level 2 and Level 5. See the text for additional details.

Figure 3. One-dimensional simulation of an evenly illuminated scene. In this and the following 1-D simulations the four graphs, from bottom to top respectively, refer to the Level 1 stimulus distribution (labeled Stimulus), the Level 2 on-cell distribution (labeled Feature), the Level 5 BC output (labeled Boundary), and the Level 6 filled-in syncytium (labeled Output). The parameters used in the simulations are listed in the Appendix.

Figure 4. Brightness constancy: The same scene as in Figure 3, but now unevenly illuminated. Although the two Stimulus distributions in Figures 3 and 4 are different, the final Output distributions are very similar.

Figure 5. Brightness contrast: The stimulus contains two medium luminance patches, the left one on a low luminance background, and the right one on a high luminance background. The Output predicts the left patch to look brighter than the right patch. In contrast, in the Feature profile, the central activity levels corresponding to the two patches are equal. Thus brightness contrast cannot be explained solely by contour generated activity, but a filling-in process is also necessary.

Figure 6. The COCE. (a) The stimulus distribution. (b) The on-cell activity profile. (c) The output of the BC System. (d) The filled-in syncytium, which predicts the brightness of the stimulus, and should be compared with Figure 1. The parameters for this and the following 2-D simulations are listed in the Appendix.

Figure 7. The Koffka-Benussi ring. (a) The stimulus distribution corresponding to the homogeneous undivided square annulus of medium luminance on a bipartite background. (b) The filled-in output corresponding to the stimulus in (a). (c) The same stimulus distribution as in (a), except that the annulus is here divided by vertical short lines into two equiluminous halves. (d) The filled-in output corresponding to the stimulus in (b). The two halves of the annulus are homogeneous and have different brightness levels.

Figure 8. The evenly illuminated Mondrian. (a) The stimulus distribution consists of 13 homogeneous polygons with 4 luminance levels. Note that the square in the upper left portion of the stimulus has the same luminance and size as the square in the lower right portion. However, the average luminance of the regions surrounding the lower square is higher than the corresponding average luminance for the upper square. (b) The on-cell distribution. The amount of on-cell activity within the upper square is higher than that within the lower square. (c) The BC output. (d) The filled-in syncytium. The upper square is correctly predicted to look brighter than the lower square.

Figure 9. The unevenly illuminated Mondrian. (a) The stimulus distribution simulates the transformation of Figure 8a caused by the presence of a light source whose intensity decreases linearly from the lower right corner toward the upper left corner of the stimulus.

The lower square is now more luminant than the upper square. (b) The on-cell distribution. (c) The BC output. (d) The filled-in syncytium. Figures 9b, 9c, and 9d are very similar to the corresponding figures for the evenly illuminated Mondrian (Figure 8). This illustrates the model's discounting of the illuminant. In addition, the upper square is still predicted to appear brighter than the lower square, a case of contrast constancy.

Figure 1

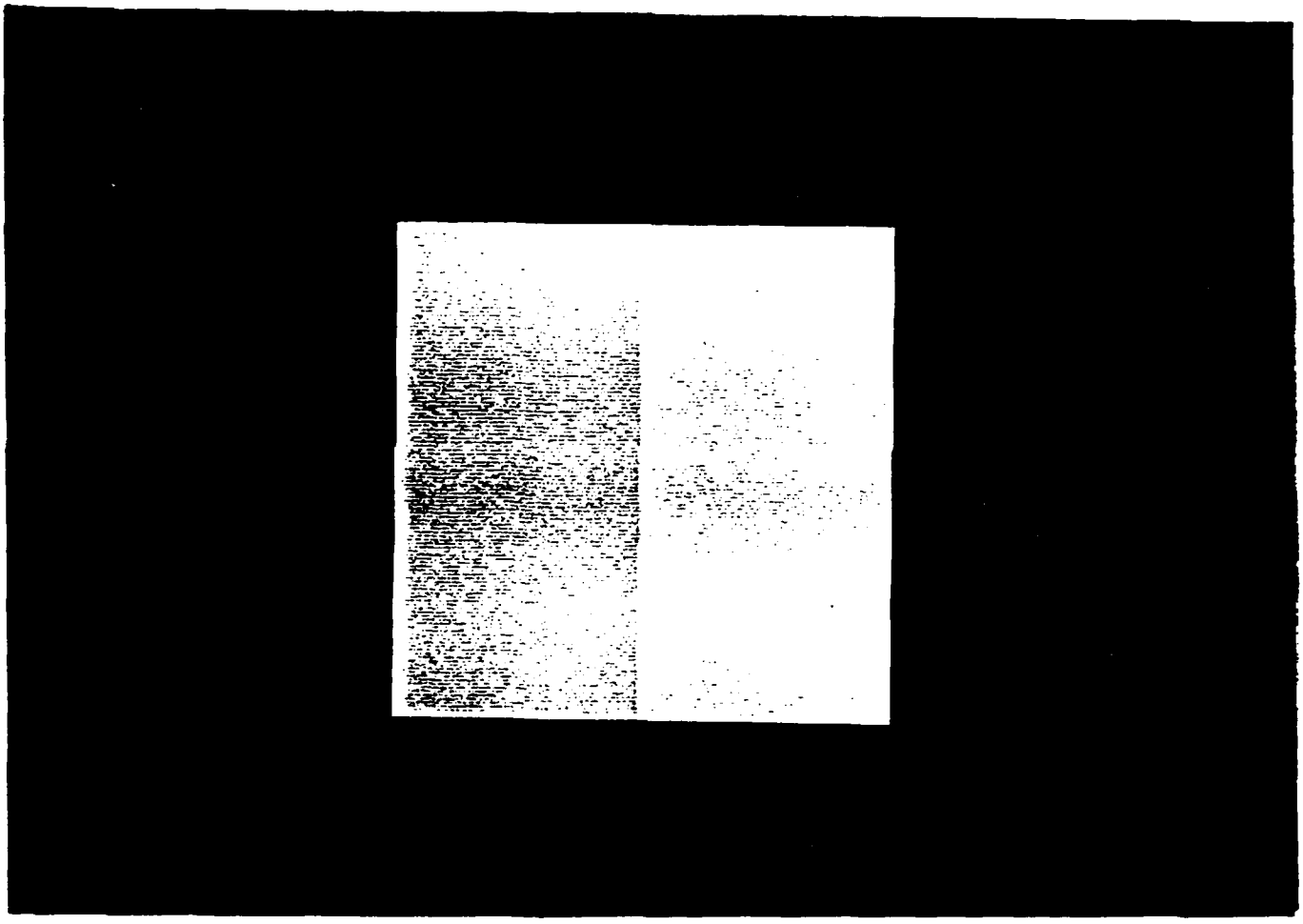

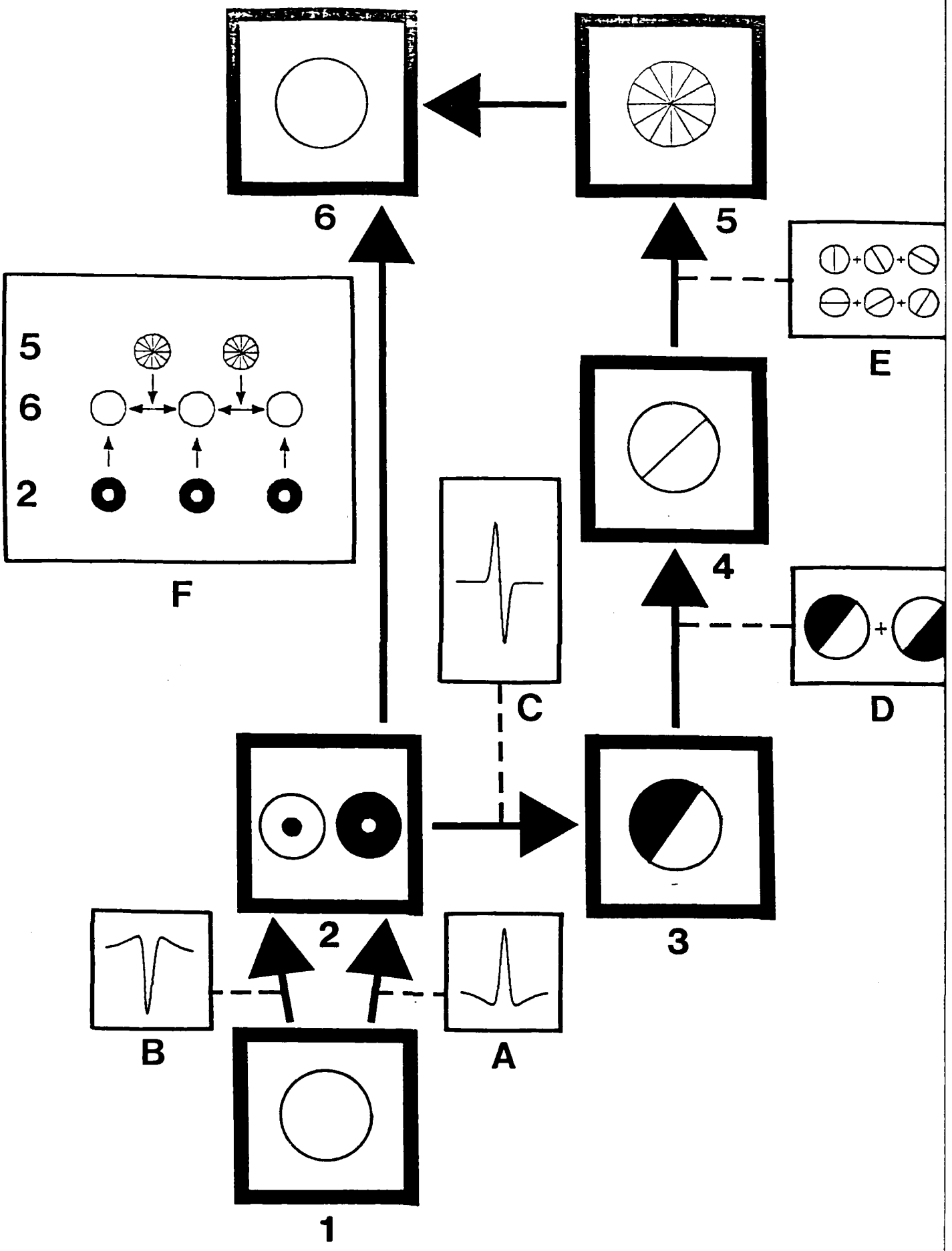
6
5
E
5
6
2
F
4
C
D
2
3
B
A
1

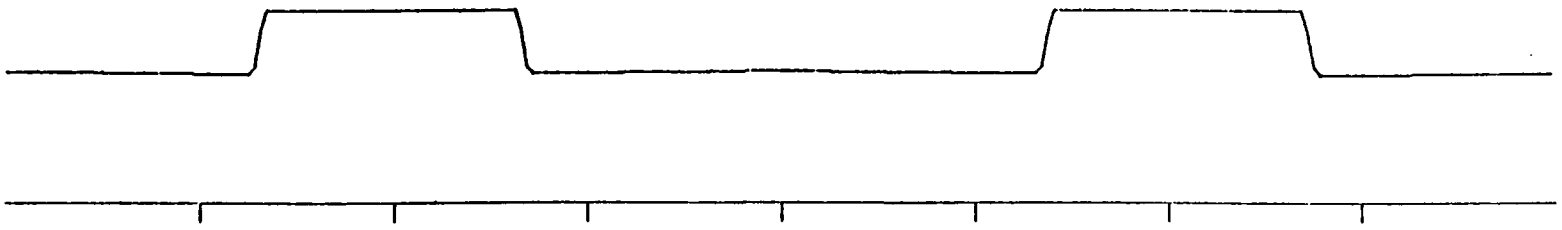

OUTPUT

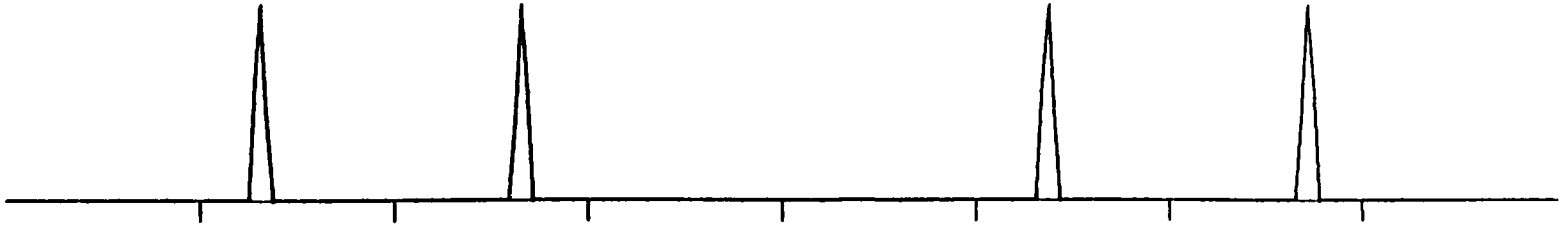

BOUNDARY

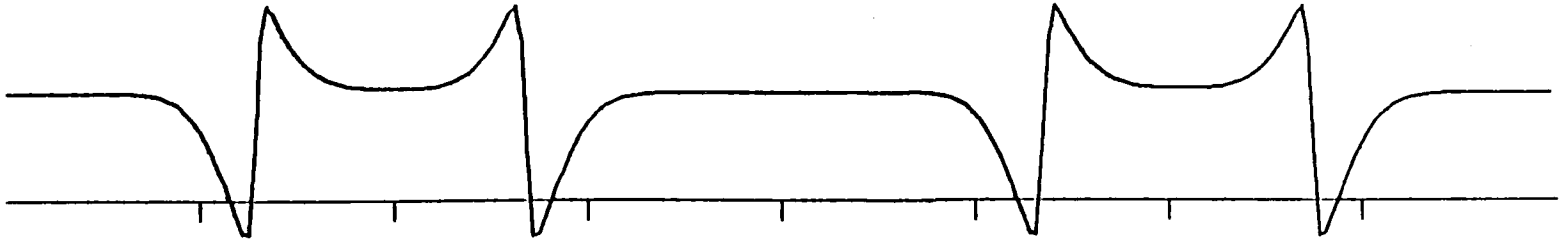

FEATURE

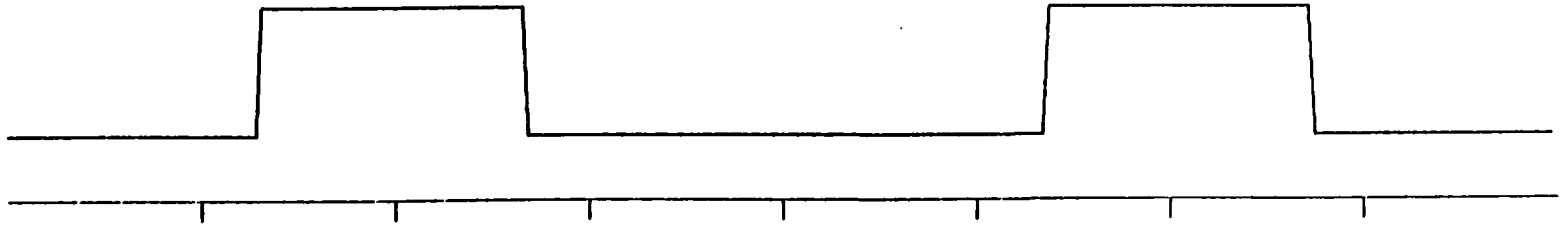

STIMULUS

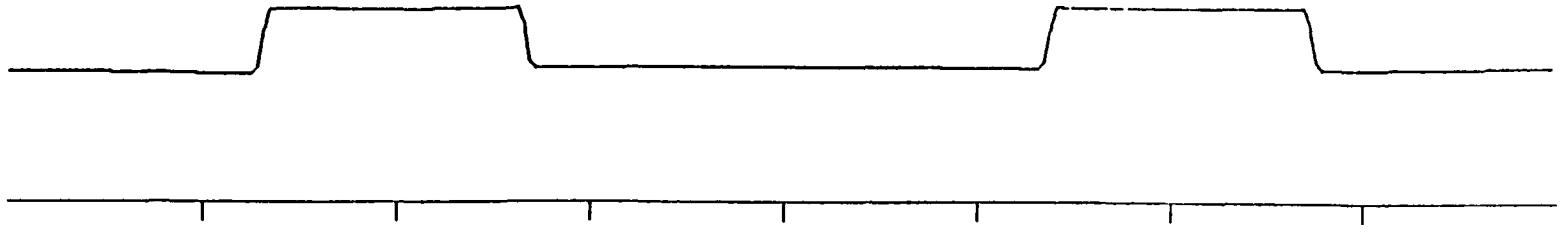

OUTPUT

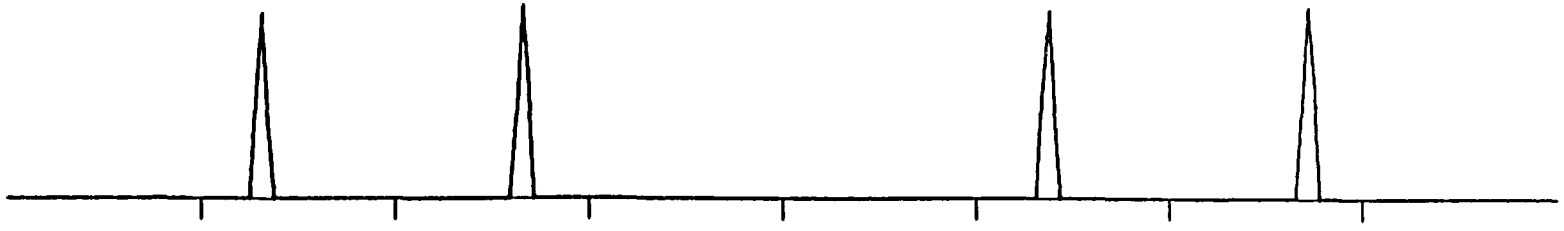

BOUNDARY

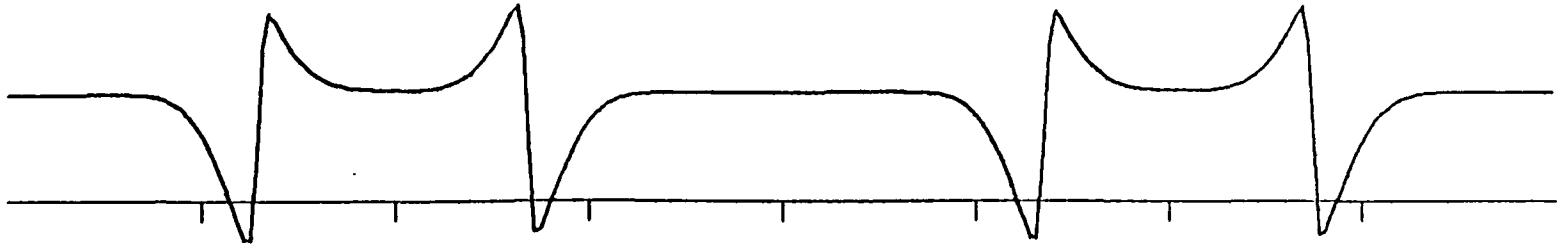

FEATURE

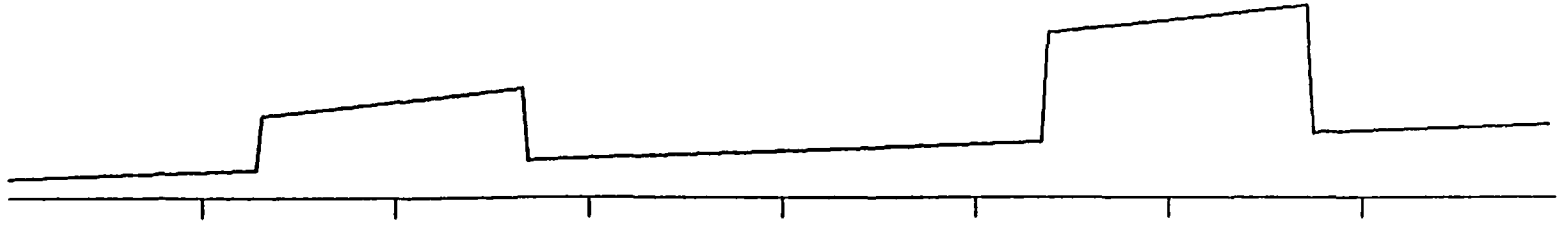

STIMULUS

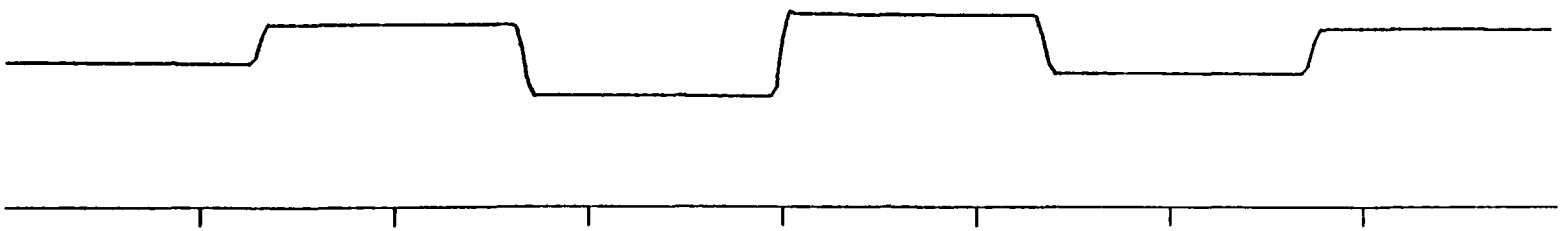

OUTPUT

BOUNDARY

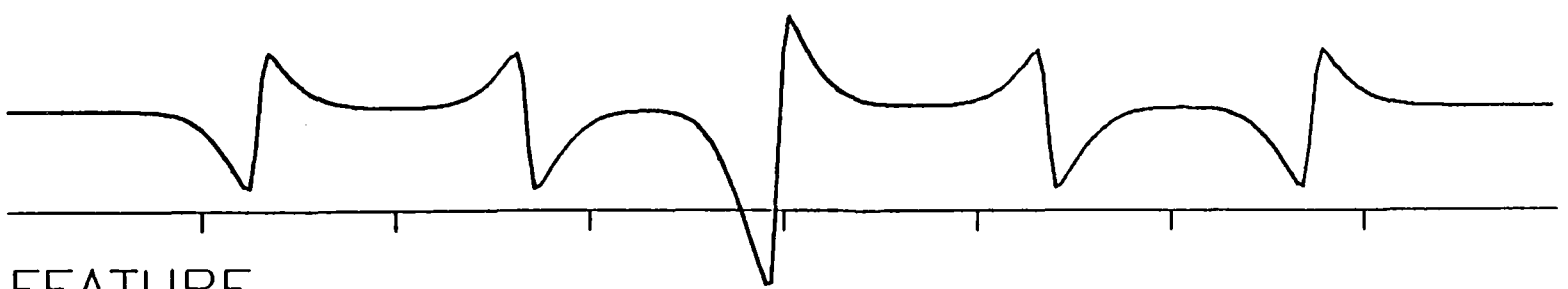

FEATURE

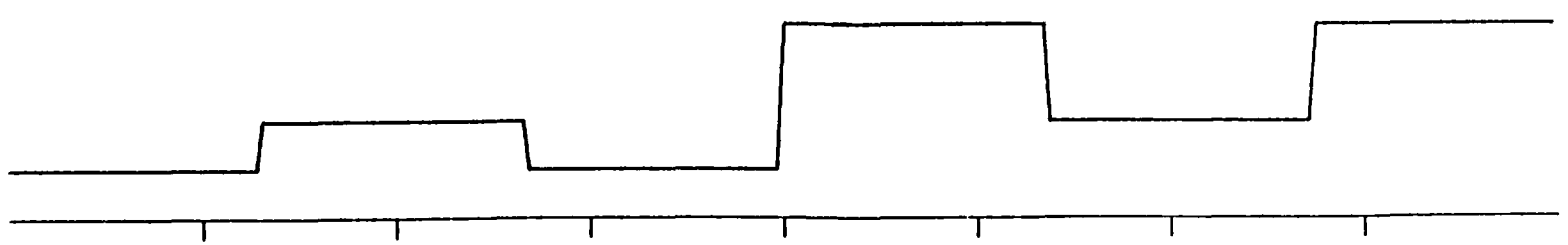

STIMULUS